Reviews on Advanced Materials and Technologies, 2024, vol. 6, no. 3, pp. 89–95
DOI: 10.17586/2687-0568-2024-6-3-89-95

Model of Ductile Fracture Initiation in Metal/Graphene Composites

N.V. Skiba*, A.G. Sheinerman

Institute for Problems in Mechanical Engineering, Russian Academy of Sciences, St. Petersburg 199178, Russia

Article history

Received July 15, 2024
Accepted July 22, 2024
Available online July 25, 2024

Abstract

We suggest a model that describes the initiation of ductile fracture in metal/graphene composites. Within the model, the cracks are generated at dislocation pileups formed at the metal/graphene interfaces in the course of plastic deformation of composites. The transformation of these cracks to elongated voids and their coalescence leads to ductile failure of metal/graphene composites. For an exemplary case of Al-4Cu/graphene composites we have calculated the critical strain for the ductile fracture initiation as a function of the structural parameters of graphene platelets. Assuming that strain to failure is mainly determined by the strain for fracture initiation, we have calculated the strain to failure of metal/graphene composites. It appeared that strain to failure is maximum in the case of short graphene platelets. The calculated values of strain to failure agree with the experimental data for Al-4Cu/graphene composites.

Keywords: Metals; Graphene; Composites; Fracture; Cracks

1. INTRODUCTION

Recently, metal/graphene composites have attracted significant interest due to their enhanced strength, electrical and thermal conductivity and corrosion resistance; see. e.g., reviews [1–20]. The incorporation of graphene into metal matrices results in materials with improved mechanical performance, wear resistance, and thermal stability, making them promising candidates for a wide range of applications in the aerospace and automotive industries, electronics, and structural engineering.

One of the key advantages of metal/graphene composites over traditional pure metals or metal alloys is their enhanced strength. Graphene in the metal matrix acts as a reinforcing phase, effectively hindering dislocation motion and facilitating the load transfer within the composite, further enhancing its mechanical properties; see, e.g., Refs. [7,18]. For example, various studies demonstrated that the addition of graphene can increase both yield and ultimate strength of metals and metal alloys [1–20]. At the same time, an increase in strength is often accompanied by a decrease in tensile ductility, which can be related either to necking or to ductile fracture. While the effect of graphene inclusions on strength is theoretically studied in various papers (see, e.g., review [18]), the effect of graphene on fracture behavior of metal/graphene composites attracted only limited attention [21–27].

For example, Jiang et al. [21] developed a cohesive zone model (CZM) to simulate the interfacial behavior between graphene coatings and Al substrate. The finite element (FE) simulations of deformation of Al/graphene composites with a progressive damage at the Al/graphene interfaces were performed by Su et al. [22] and Song et al. [23]. These models, however, only examined fracture in terms of adhesion of the metal matrix and graphene and did not consider the microstructure of the metal matrix as well as the crack initiation and propagation at grain boundaries and inside grains. Liu et al. [24] combined the crystal plasticity FE modeling with the CZM to simulate the damage evolution of the deformed Al/graphene composites. The works [25–27] combined the mechanism-based theoretical stress-strain relations of metal/graphene composites with the description of a process of damage accumulation characterized by a damage parameter. However, the studies [24,27] did not reveal the relation between the strain to failure and the structural parameters of the composites. The authors of work [26] predicted that the strain to failure should increase with a decrease in the thickness

* Corresponding author: N.V. Skiba, e-mail: nikolay.skiba@gmail.com

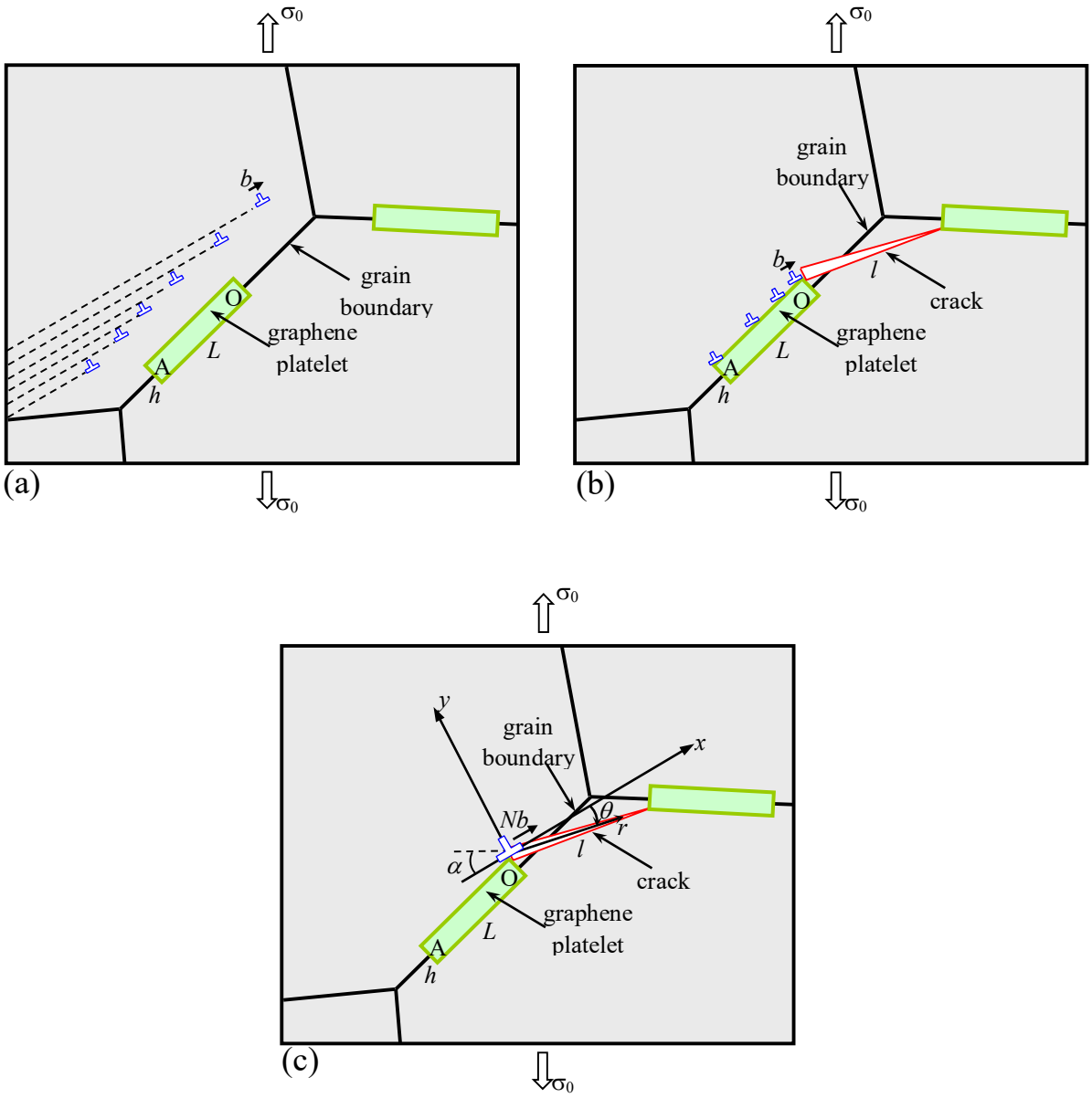

Fig. 1. Model of the ductile failure of a metal/graphene composite. (a) Lattice dislocations slip across the grain. (b) Formation of a dislocation pile-up AO at the boundary of the graphene platelet and the matrix, and generation of a crack with length l at the dislocation pile-up. (c) The dislocation pileup AO is modeled by a superdislocation with the Burgers vector magnitude Nb.

to length ratio of graphene platelets, while Ref. [25] confirmed that the strain to failure of Cu/graphene composites reduces with an increase in the graphene volume fraction. At the same time, the above studies did not examine the exact mechanism of fracture initiation and propagation. The aim of the present study is to suggest a model of ductile fracture initiation in metal/graphene composites and to reveal the dependences of the strain to failure of such composites on the structural parameters of graphene platelets.

2. MODEL

Let us consider a deformed composite solid under the action of a uniaxial tensile mechanical load σ_0. Within the model, the solid consists of a matrix based on a metallic alloy and graphene platelets located along grain boundaries (GBs). Graphene platelets are modeled as disks with a diameter L and thickness h and their average lateral size is assumed to be smaller than the characteristic GB length (Fig. 1a).

Following the results [28] on the ductile fracture of Al2024/graphene composites, we assume that the ductile fracture of metal/graphene composites occurs via the generation of cracks or voids at graphene platelets and the propagation of cracks to other graphene platelets. Within this approach, we suppose that ductile fracture occurs via the formation of cracks near graphene platelets. These cracks transform to elongated pores. If their length is close to the distance between neighboring graphene platelets,

these pores can coalesce resulting in ductile failure. We also assume that after the initiation of the initial cracks with sufficient lengths near graphene platelets, subsequent failure through the transformation of these cracks to pores and their coalescence proceeds very quickly. As a result, strain to failure can be approximated by the critical strain for the formation of a crack that is stretched from one graphene platelet to another.

Consider an individual graphene platelet AO at a GB (Fig. 1a). Under the action of the mechanical load σ_0, lattice dislocations with the Burgers vectors **b** slip in the grain interior and stop at graphene platelets and GBs (Fig. 1a). Following the results of experiment [29], we assume that the slipping lattice dislocations are accumulated at graphene platelets, while they are not accumulated at graphene-free parts of GBs due to the fast recovery (Fig. 1b). As a result, a pile-up of edge dislocations with the identical Burgers vectors $b = a\sqrt{2}/2$ (where a is the lattice parameter) is formed at the boundary AO of the graphene platelet and the matrix, and is fixed at the edge of the graphene platelet at point O (Fig. 1b).

Next, consider generation of a nanocrack with a length l at the dislocation pile-up near edge O of the graphene platelet in the sum stress field of the dislocation pile-up and the external load σ_0 (Fig. 1b). In the following, we focus on the case of short graphene platelets, where the crack length l is much greater than the platelet length L.

In this case, for the calculation of the equilibrium crack length l, the dislocation pileup AO will be modeled by a superdislocation with the Burgers vector magnitude Nb (Fig. 1c), where N is the number of dislocations in the pileup. Within the model, the Burgers vector of the superdislocation makes an angle α with the normal to the direction of the applied load σ_0 (Fig. 1c).

Let us calculate the critical length l of the nanocrack. To do so, we introduce the polar coordinate system (r, θ) associated with the crack with the origin at the point O as shown in Fig. 1c. In the framework of the model, the nanocrack opens under action of the normal, $\sigma^0_{\theta\theta}(r,\theta)$ and $\sigma^b_{\theta\theta}(r,\theta)$, and shear, $\sigma^0_{r\theta}(r,\theta)$ and $\sigma^b_{r\theta}(r,\theta)$, components of the stress fields created by the external load ($\sigma^0_{i\theta}$) and the superdislocation ($\sigma^b_{i\theta}$). To calculate these components, we use the Cartesian coordinate system (x, y) (Fig. 1c) and the well-known stress components of the superdislocation [30]:

$$\sigma^b_{xx} = -DNb\frac{y(3x^2+y^2)}{(x^2+y^2)^2},$$

$$\sigma^b_{yy} = DNb\frac{y(x^2-y^2)}{(x^2+y^2)^2},$$

$$\sigma^b_{xy} = DNb\frac{x(x^2-y^2)}{(x^2+y^2)^2}, \quad (1)$$

where $D = G/[2\pi(1-\nu)]$, G is the shear modulus, and ν is the Poisson ratio.

Using formula (1) and the coordinate transformations $x = r\cos\theta$ and $y = -r\sin\theta$, we can rewrite the stress components $\sigma^b_{\theta\theta}(r,\theta)$ and $\sigma^b_{r\theta}(r,\theta)$ as follows:

$$\sigma^b_{\theta\theta}(r,\theta) = \sigma^b_{xx}\sin^2\theta + \sigma^b_{yy}\cos^2\theta + \sigma^b_{xy}\sin 2\theta, \quad (2)$$

$$\sigma^b_{r\theta}(r,\theta) = (\sigma^b_{xx} - \sigma^b_{yy})\sin\theta\cos\theta + \sigma^b_{xy}\cos 2\theta. \quad (3)$$

The components of the stress created by the external load σ_0 in the plane of the nanocrack are expressed as

$$\sigma^0_{\theta\theta}(r,\theta) = \sigma_0\cos^2(\alpha-\theta), \quad (4)$$

$$\sigma^0_{r\theta}(r,\theta) = \sigma_0\sin 2(\alpha-\theta), \quad (5)$$

To characterize quantitatively the conditions of the nanocrack generation, let us calculate in the first approximation the critical length l of the nanocrack. To do so, we will use the following condition of crack growth [31] $F \geq 2\gamma$, which gives the balance between the strain energy release rate F associated with crack growth and the specific energy of the formation of two new nanocrack surfaces characterized by the surface energy γ per unit area.

The energy release rate can be written as [31]

$$F = \frac{\pi(1-\nu)l}{4G}(\bar{\sigma}^2_{\theta\theta} + \bar{\sigma}^2_{\theta\theta}), \quad (6)$$

where $\bar{\sigma}_{\theta\theta}$ and $\bar{\sigma}_{r\theta}$ are the mean weighted values of the sum stress components $\sigma_{\theta\theta}(r,\theta) = \sigma^0_{\theta\theta}(r,\theta) + \sigma^b_{\theta\theta}(r,\theta)$ and $\sigma_{r\theta}(r,\theta) = \sigma^0_{r\theta}(r,\theta) + \sigma^b_{r\theta}(r,\theta)$, respectively. These mean weighted values are determined by the following formulas [31]:

$$\bar{\sigma}_{\theta\theta} = \frac{2}{\pi l}\int_0^l \sigma_{\theta\theta}(r,\theta)\sqrt{\frac{r}{l-r}}dr, \quad (7)$$

$$\bar{\sigma}_{r\theta} = \frac{2}{\pi l}\int_0^l \sigma_{r\theta}(r,\theta)\sqrt{\frac{r}{l-r}}dr. \quad (8)$$

When a nanocrack forms in the stress field of a superdislocation, its growth is energetically favored until its length reaches an equilibrium length l_e, which can be found from the critical condition $F(l = l_e) = 2\gamma$ [31]. Substituting formula (6) to the latter condition, we obtain

$$\frac{8G\gamma}{\pi(1-\nu)l_e} = \bar{\sigma}^2_{\theta\theta} + \bar{\sigma}^2_{r\theta}. \quad (9)$$

3. RESULTS

With the help of formulae (1)–(5) and (7)–(9), we can relate the parameter N to the equilibrium nanocrack length l_e. Following [28], we assume that ductile failure occurs via the generation of cracks at graphene platelets,

their transformation to pores and coalescence. Under this assumption, we postulate that ductile failure can occur if the nanocrack is large enough to connect to neighboring graphene platelets. This can be the case if its equilibrium length is not smaller than the average distance between graphene platelets. Thus, the critical condition for ductile failure can be written as $l_e = l_0$, where l_0 is the distance between the edges of the neighboring graphene platelets.

According to the work [32], the average distance between the edges of neighboring graphene platelets can be expressed as

$$l_0(f_v) = \pi\sqrt{\frac{Lh}{8f_v}} - \frac{4L}{\pi^2}, \tag{10}$$

where f_v is the volume fraction of the graphene platelets.

In our case, the number N of the dislocations at the graphene platelets depending on the true plastic strain ε_p is given by the formula [33]:

$$N = \alpha_0 L n^* \left[1 - \exp\left(\frac{-\beta_0 M}{bn^*}\varepsilon_p\right)\right], \tag{11}$$

where $\alpha_0 < 1$ is a parameter that takes into account the presence of dislocations at the lower boundary of the graphene platelet, $\beta_0 \approx 1$ is the geometric factor, $M \approx 3$ is the Taylor factor and n^* is the model parameter that has the meaning of the maximum number of dislocations that can be accumulated at the graphene platelet.

Thus, the true plastic strain can be expressed from formula (11) as follows:

$$\varepsilon_p = -\frac{bn^*}{\beta_0 M}\ln\left(1 - \frac{N}{\alpha n^* L}\right). \tag{12}$$

Within the framework of the model, it is assumed that the ductile fracture of the composite occurs when a crack of length l_0 is formed at the dislocation pileup. This occurs when a critical number N_c of the dislocations is accumulated at the graphene platelet boundary. In this situation, the critical true plastic strain for ductile failure ε_c is defined as $\varepsilon_c = \varepsilon_p(N = N_c)$, where $N_c = N\big|_{l=l_0(f_v)}$.

Then, using the equality $\varepsilon_e = \exp(\varepsilon_p) - 1$ that relates the engineering plastic strain ε_e with the true plastic strain ε_p, we can relate the critical true plastic strain $\varepsilon_c(f_v, L)$ to the critical engineering plastic strain to failure $\varepsilon_e^c(f_v, L) = \varepsilon_e(\varepsilon_p = \varepsilon_c)$.

At first, let us calculate the dependence the critical number dislocations N_c on the azimuthal angle θ in the exemplary case of Al-4Cu/graphene composite. The material parameters are as follows: $G = 28$ GPa, $\nu = 0.33$, $\gamma \approx 1.5$ J/m^2. The external true stress σ_0 was chosen to be 300 MPa, which corresponds to the average ultimate true stress obtained in the experimental work [34] for Al-4Cu/graphene composite. We accept this assumption since the critical plastic strain weakly depends on the external stress σ_0. The length L and the thickness h were taken as 100 nm and 10 nm, respectively. In the following, we focus on the case of sufficiently small graphene volume fraction, for which the relation $L << l_0$ required for the replacement of the dislocation pileup by a superdislocation (Fig. 1b,c) is satisfied. The dependences $N_c(\theta)$ for $\alpha = 45°$ and various values of the graphene volume fraction f_v are shown in Figure 2. As follows from Fig. 2, crack nucleation is most favorable at the angle $\theta \approx 45°$.

Now let us calculate the dependences of the engineering strain to failure ε_e^c on the graphene volume fraction f_v

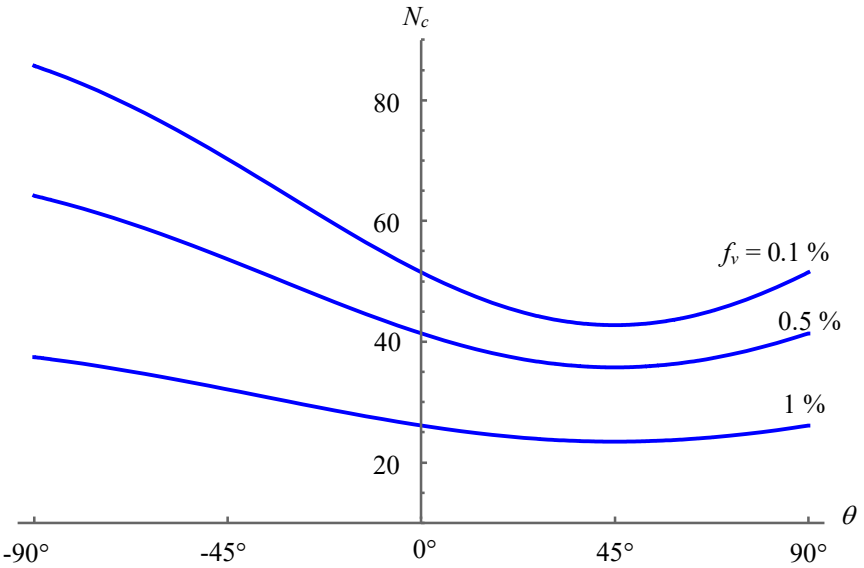

Fig. 2. Dependences of the critical number of dislocations N_c on the azimuthal angle θ for various values of the graphene volume fraction f_v.

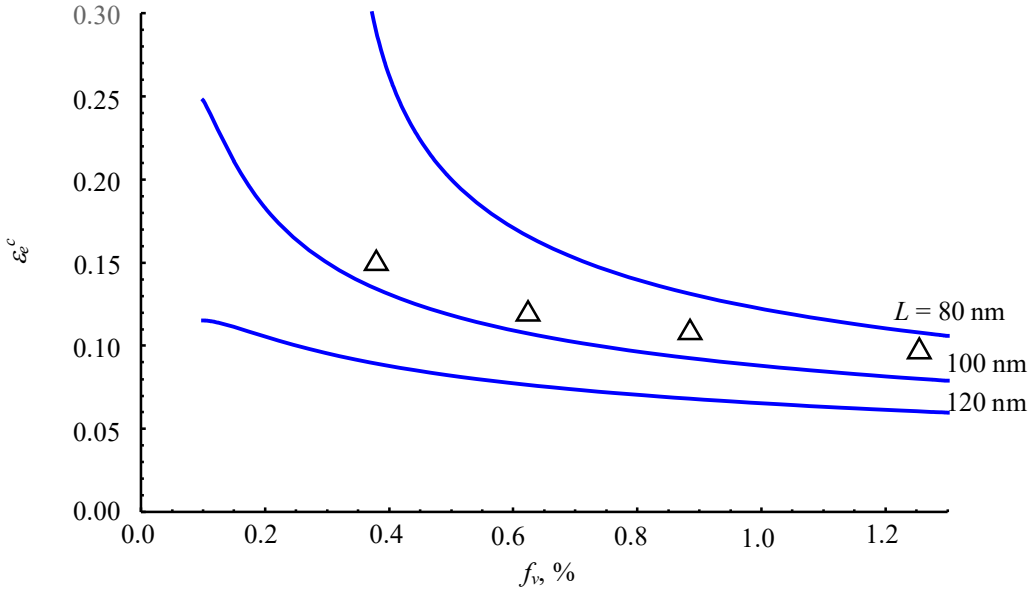

Fig. 3. Dependences the engineering strain to failure ε_e^c on the graphene volume fraction f_v for various values of the graphene platelet length L. Triangles correspond to the experimental data from work [34].

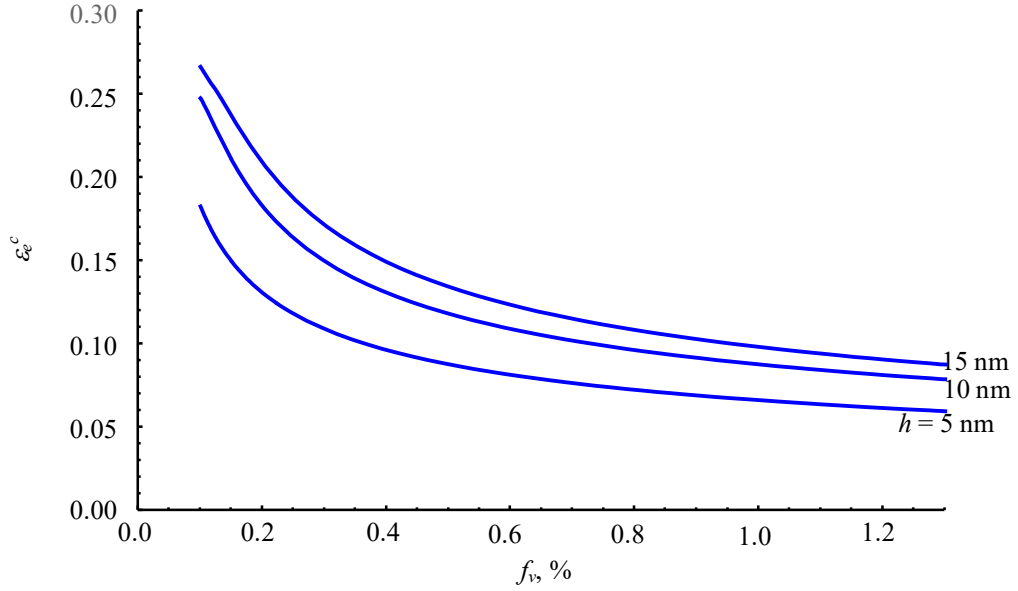

Fig. 4. Dependences the engineering strain to failure ε_e^c on the graphene volume fraction f_v for various values of the graphene platelet thickness h.

for various values of the length L and the thickness h, using the same parameters as above and the parameters $\alpha_0 = 0.8$ and $n^* = 0.7$ nm^{-1} as the fitting parameters. The dependences $\varepsilon_e^c(f_v)$ are shown in Figure 3 at $h = 10$ nm and in Figure 4 at $L = 100$ nm. These dependences demonstrate good agreement with experimental data [34] at values of the length $L = 100$ nm and the thickness $h = 15$ nm. It is seen from Figs. 3 and 4 that the engineering strain to failure ε_e^c decreases with an increase in the graphene volume fraction f_v. For a preset graphene volume fraction f_v, ε_e^c increases with a decrease in the graphene platelet length L and an increase in their thickness h. An increase in the strain to failure ε_e^c with graphene platelet thickness h can be explained by the fact that for a specified volume fraction of graphene, an increase in the platelet thickness leads to a decrease in the number density of graphene platelets. This implies an increase in the average distance between graphene platelets, and, as a result, a rise in the critical crack length l_0 for the onset of ductile failure. Also, an increase in the strain to failure with a decrease in the graphene platelet length L can be associated with a decrease in the number of dislocations accumulated at

each graphene platelet at a given plastic strain. The smaller number of dislocations at the platelets provides smaller stress concentration. This hinders the growth of nanocracks near graphene platelets and thereby increases strain to failure.

4. CONCLUSIONS

Thus, we have suggested a theoretical model that enables one to calculate the strain to failure of metal/graphene composites for the case where these composites fail due to ductile fracture. Within the model, ductile fracture occurs via the formation of cracks near graphene platelets, their transformation to pores and subsequent coalescence. For the exemplary cases of Al-4Cu/graphene composites it is demonstrated that strain to failure decreases with an increase with the graphene platelet volume fraction. This can be explained by a reduction of the distance between graphene platelets with an increase of the graphene volume fraction, which facilitates the propagation of cracks between graphene platelets. The calculations also demonstrate that at a specified volume fraction of graphene, the strain to failure in the case of ductile fracture is maximum for short graphene platelets.

ACKNOWLEDGEMENTS

The authors acknowledge the support of the Russian Foundation for Basic Research (grant 20-53-56036).

REFERENCES

[1] S.C. Tjong, Recent progress in the development and properties of novel metal matrix nanocomposites reinforced with carbon nanotubes and graphene nanosheets, *Mater. Sci. Eng. R*, 2013, vol. 74, no. 10, pp. 281–350.

[2] I.A. Ovid'ko, Metal-graphene nanocomposites with enhanced mechanical properties: a review, *Rev. Adv. Mater. Sci.*, 2014, vol. 38, no. 2, pp. 190–200.

[3] A. Nieto, A. Bisht, D. Lahiri, C. Zhang, A. Agarwal, Graphene reinforced metal and ceramic matrix composites: a review, *Int. Mater. Rev.*, 2017, vol. 62, no. 5, pp. 241–302.

[4] Z. Hu, G. Tong, D. Lin, C. Chen, H. Guo, J. Xu, L. Zhou, Graphene-reinforced metal matrix nanocomposites – a review, *Mater. Sci. Technol.*, 2016, vol. 32, no. 9, pp. 930–953.

[5] I.A. Kinloch, J. Suhr, J. Lou, R.J. Young, P.M. Ajayan, Composites with carbon nanotubes and graphene: An outlook, *Science*, 2018, vol. 362, no. 6414, pp, 547–553.

[6] A. Saboori, M. Dadkhah, P. Fino, M. Pavese, An overview of metal matrix nanocomposites reinforced with graphene nanoplatelets; mechanical, electrical and thermophysical properties, *Metals*, 2018, vol. 8, no. 6, art. no. 423.

[7] P. Hidalgo-Manrique, X. Lei, R. Xu, M. Zhou, I.A. Kinloch, R.J. Young, Copper/graphene composites: a review, *J. Mater. Sci.*, 2019, vol. 54, pp, 12236–12289.

[8] N. Seyed Pourmand, H. Asgharzadeh, Aluminum matrix composites reinforced with graphene: A review on production, microstructure, and properties, *Crit. Rev. Solid State Mater. Sci.*, 2019, vol. 45, no. 4, pp. 289–337.

[9] Ö Güler, N. Bağcı, A short review on mechanical properties of graphene reinforced metal matrix composites, *J. Mater. Res. Technol.*, 2020, vol. 9, no. 3, pp. 6808–6833.

[10] S.I. Ahmad, H. Hamoudi, A. Abdala, Z.K. Ghouri, K.M. Youssef, Graphene-reinforced bulk metal matrix composites: Synthesis, microstructure, and properties, *Rev. Adv. Mater. Sci.*, 2020, vol. 59, pp. 67–114.

[11] X. Zhang, N. Zhao, C. He, The superior mechanical and physical properties of nanocarbon reinforced bulk composites achieved by architecture design – A review, *Prog. Mater. Sci.*, 2020, vol. 113, art. no.100672.

[12] M. Yang, Y. Liu, T. Fan, D. Zhang, Metal-graphene interfaces in epitaxial and bulk systems: A review, *Prog. Mater. Sci.*, 2020, vol. 110, art. no. 100652.

[13] M. Tabandeh-Khorshid, K. Ajay, E. Omrani, C. Kim, P. Rohatgi, Synthesis, characterization, and properties of graphene reinforced metal-matrix nanocomposites, Composites B, 2020, vol. 183, art. no. 107664.

[14] Z.Y. Zhao, P.K. Bai, W.B. Du, B. Liu, D. Pan, R. Das, C.T. Liu, Z.H. Guo, An overview of graphene and its derivatives reinforced metal matrix composites: Preparation, properties and applications, *Carbon*, 2020, vol. 170, pp. 302–326.

[15] V. Khanna, V. Kumar, S.A. Bansal, Mechanical properties of aluminium-graphene/carbon nanotubes (CNTs) metal matrix composites: Advancement, opportunities and perspective, *Mater Res. Bull.*, 2021, vol. 138, art. no. 111224.

[16] J. Su, J. Teng, Recent progress in graphene-reinforced aluminum matrix composites, *Front. Mater. Sci.*, 2021, vol. 15, pp. 79–97.

[17] P. Lava Kumar, A. Lombardi, G. Byczynski, S.V.S. Narayana Murty, B.S. Murty, L. Bichler, Recent advances in aluminium matrix composites reinforced with graphene-based nanomaterial: A critical review, *Prog. Mater. Sci.*, 2022, vol. 128, art. no. 100948.

[18] A.G. Sheinerman, Plastic deformation and fracture processes in metal/graphene composites: a review, *Crit. Rev. Solid State Mater. Sci.*, 2022, vol. 47, no. 5, pp. 708–735.

[19] A.G. Sheinerman, Mechanical properties of metal matrix composites with graphene and carbon nanotubes, *Phys. Metal. Metallogr.*, 2022, vol. 123, pp. 57–84.

[20] M.A. Alam, H.B. Ya, M. Azad, M. Azeem, M. Mustapha, M. Yusuf, F. Masood, R.V. Marode, S.M. Sapuan, A.H. Ansari, Advancements in aluminum matrix composites reinforced with carbides and graphene: A comprehensive review, *Nanotechnol. Rev.*, 2023, vol. 12, art. no. 20230111.

[21] W.G. Jiang, Y. Wu, Q.H. Qin, D.S. Li, X.B. Liu, M.F. Fu, A molecular dynamics based cohesive zone model for predicting interfacial properties between graphene coating and aluminum. *Comput. Mater. Sci.,* 2018, vol. 151, pp. 117–123.

[22] Y. Su, Z. Li, Y. Yu, L. Zhao, Z. Li, Q. Guo, Composite structural modeling and tensile mechanical behavior of graphene reinforced metal matrix composites, *Sci. China Mater.*, 2018, vol. 61, pp. 112–124.

[23] Y. Song, Y. Ma, K. Zhan, Simulations of deformation and fracture of graphene reinforced aluminium matrix nano-laminated composites, *Mech. Mater.*, 2020, vol. 142, art. no. 103283.

[24] L.-Y. Liu, Q.-S. Yang, X. Liu, J.-J. Shang, Modeling damage evolution of graphene/aluminum composites considering crystal cracking and interface failure, *Composite Structures*, 2021, vol. 267, art. no. 113863.

[25] X.D. Xia, Y. Su, Z. Zhong, G.J. Weng, A unified theory of plasticity, progressive damage and failure in graphene-metal nanocomposites, *Int. J. Plast.*, 2017, vol. 99, pp. 58–80.
[26] Y. Sun, A. Li, Y.F. Hu, X.H. Wang, M.B. Liu, Simultaneously enhanced strength-plasticity of graphene/metal nanocomposites via interfacial microstructure regulation, *Int. J. Plast.*, vol. 148, art. no. 103143.
[27] Y. Sun, A. Li, W. Zhang, M. Liu, Theoretical framework to predict the balance of strength-ductility in graphene/metal nanocomposites, *Int. J. Solids Struct.*, 2023, vol. 268, art. no. 112182.
[28] S.E. Shin, D.H. Bae, Deformation behavior of aluminum alloy matrix composites reinforced with few-layer graphene, *Composites A*, 2015, vol. 78, pp. 42–47.
[29] Y. Jiang, R. Xu, Z. Tan, G. Ji, G. Fan, Z. Li, D.-B. Xiong, Q. Guo, Z. Li, D. Zhang, Interface-induced strain hardening of graphene nanosheet/aluminum composites, *Carbon*, 2019, vol. 146, pp. 17–27.
[30] A.E. Romanov, V.I. Vladimirov, *Disclinations in crystalline solids*, in: F.R.N. Nabarro (Ed.), *Dislocations in Solids*, North-Holland, Amsterdam, 1992, pp. 191–402.
[31] V.L. Indenbom, Criteria of fracture in dislocation theories of strength, *Phys. Stat. Solidi*, 1961, vol. 3, no. 7, pp. 2071–2079.
[32] A.G. Sheinerman, M.Yu. Gutkin, Model of enhanced strength and ductility of metal/graphene composites with bimodal grain size distribution, *Metall. Mater. Trans. A*, 2020, vol. 51, pp. 189–199.
[33] S.V. Bobylev, A.G. Sheinerman, X.T. Li, Z.J. Zhang, Modeling of strength and ductility of metal alloy/graphene composites containing precipitates. *Int. J. Solids Struct.*, 2024, vol. 296, art. no. 112843.
[34] M. Khoshghadam-Pireyousefan, R. Rahmanifard, L. Orovcik, P. Švec, V. Klemm, Application of a novel method for fabrication of graphene reinforced aluminum matrix nanocomposites: Synthesis, microstructure, and mechanical properties, *Mater. Sci. Eng. A*, 2020, vol. 772, art. no. 138820.

УДК 53.091

Модель начала вязкого разрушения композитов «металл/графен»

Н.В. Скиба, А.Г. Шейнерман

Институт проблем машиноведения РАН, Санкт-Петербург 199178, Россия

Аннотация. Предложена модель, описывающая начальную стадию вязкого разрушения в композитах «металл/графен». В рамках модели трещины зарождаются в поле напряжений дислокационных скоплений, образующихся на границах раздела «металл/графен» в процессе пластической деформации композитов. Преобразование этих трещин в удлиненные поры и их слияние приводит к вязкому разрушению композитов «металл/графен». Для случая композитов Al-4Cu/графен рассчитана критическая деформация для начала вязкого разрушения в зависимости от структурных параметров графеновых пластинок. Предполагая, что деформация до разрушения в основном определяется деформацией, при которой вязкое разрушения начинается, мы рассчитали деформацию до разрушения композитов «металл/графен». Оказалось, что деформация до разрушения максимальна в случае коротких графеновых пластинок. Рассчитанные значения деформации до разрушения согласуются с экспериментальными данными для композитов Al-4Cu/графен.

Ключевые слова: металлы; графен; композиты; разрушение; трещины